11-2015

Influence of Mn Concentration on Magnetic Topological Insulator MnxBi2−xTe3 Thin-Film Hall-Effect Sensor

Ravi L. Hadimani
Iowa State University and Ames Laboratory, hadimani@iastate.edu

S. Gupta
Ames Laboratory

S. M. Harstad
Ames Laboratory

Vitalij K. Pecharsky
Iowa State University and Ames Laboratory, vitkp@ameslab.gov

David C. Jiles
Iowa State University and Ames Laboratory, dcjiles@iastate.edu

Influence of Mn Concentration on Magnetic Topological Insulator MnxBi2−xTe3 Thin-Film Hall-Effect Sensor

Abstract
Hall-effect (HE) sensors based on high-quality Mn-doped Bi2Te3 topological insulator (TI) thin films have been systematically studied in this paper. Improvement of Hall sensitivity is found after doping the magnetic element Mn into Bi2Te3. The sensors with low Mn concentrations, MnxBi2-xTe3, x = 0.01 and 0.08 show the linear behavior of Hall resistance with sensitivity about 5 Ω/T. And their Hall sensitivity shows weak dependence on temperature. For sensors with high Mn concentration (x = 0.23), the Hall resistance with respect to magnetic field shows a hysteretic behavior. Moreover, its sensitivity shows almost eight times as high as that of the HE sensors with low Mn concentration. The highest sensitivity can reach 43 Ω/T at very low magnetic field. This increase of Hall sensitivity is caused by the occurrence of anomalous HE (AHE) after ferromagnetic phase transition. Our work indicates that the magnetic-element-doped TIs with AHE are good candidates for HE sensors.

Keywords
Hall-effect (HE) devices, sensitivity, thin films, topological insulators (TIs)

Comments
This is a manuscript of an article published as Ni, Y., Z. Zhang, I. C. Nlebedim, R. L. Hadimani, and D. C. Jiles. "Influence of Mn Concentration on Magnetic Topological Insulator Mn x Bi 2− x Te 3 Thin-Film Hall-Effect Sensor." IEEE Transactions on Magnetics 51, no. 11 (2015): 1-4. DOI: 10.1109/TMAG.2015.2444378. Posted with permission.

Influence of Mn Concentration on Magnetic Topological Insulator $Mn_xBi_{2-x}Te_3$ Thin Film Hall Effect Sensor

Y. Ni[1], Z. Zhang[1], I. C. Nlebedim[2,1], R. L. Hadimani[1], and D. C. Jiles[1], *Fellow, IEEE*

[1] Department of Electrical and Computer Engineering, Iowa State University, Ames, IA 50011 USA
[2] Ames Laboratory, U.S. Department of Energy

Hall-effect (HE) sensors based on high-quality Mn-doped $\mathbf{Bi_2Te_3}$ topological insulator (TI) thin films have been systematically studied in this paper. Improvement of Hall sensitivity is found after doping the magnetic element Mn into $\mathbf{Bi_2Te_3}$. The sensors with low Mn concentrations, $Mn_xBi_{2-x}Te_3$, x = 0.01 and 0.08 show the linear behavior of Hall resistance with sensitivity about **5 Ω/T**. And their Hall sensitivity shows weak dependence on temperature. For sensors with high Mn concentration (x = 0.23), the Hall resistance with respect to magnetic field shows a hysteretic behavior. Moreover, its sensitivity shows almost eight times as high as that of the HE sensors with low Mn concentration. The highest sensitivity reached **43 Ω/T** at low magnetic field strength. This increase of Hall sensitivity is caused by the occurrence of anomalous HE (AHE) after ferromagnetic phase transition. Our work indicates that the magnetic-element-doped TIs with AHE are good candidates for HE sensors.

***Index Terms*— Hall effect devices, topological insulators, thin films, sensitivity.**

I. Introduction

Hall effect sensors are used widely in areas including position sensing, DC current transformers, and fuel level indicator due to their low costs, high reliability, free of contact bounce, and immune to environmental contaminants [1]. However, the low measuring accuracy and sensitivity comparing to fluxgate magnetometers limit their applications. As a result, improving the sensitivity becomes a crucial issue for Hall effect sensors. The key factors controlling sensitivity as well as the power consumption of Hall effect sensors are carrier density and carrier mobility. Therefore, semiconductors such as GaAs and InAs with higher carrier mobility and lower carrier density than metals are often used to design Hall effect sensors [2]. In addition, anomalous Hall effect (AHE), which generates extra voltage across the current-carrying magnetic material due to spin-polarized electrons, is also used to make Hall sensors because of its robustness and improved Hall sensitivity.

Recently, a new kind of semiconductor was discovered as topological insulators (TIs), which can possess an ultra-high carrier mobility at the surface, while keep insulating in bulk [3]. The reason of high carrier mobility is that TIs have spin-polarized massless Dirac surface state. Such state, protected by time reversal symmetry, suppresses the backscattering of charge carriers upon non-magnetic impurities. Moreover, Fermi level of TIs can be tuned to the surface Dirac point which enables to reduce the density of charge carriers [4]. As a result, the ultrahigh mobility and low density of charge carriers enable TIs suitable materials for developing Hall effect sensors. In addition, introducing magnetic impurities such as Fe [5], Cr [6-8], and Mn[9-12] into TIs can introduce ferromagnetism and open a surface energy gap, which leads to interesting behaviors including magnetoelectric effect and quantized AHE[13]. As a result, TIs can also be considered as good candidates for AHE-based sensors by changing them into magnetic materials through incorporating magnetic impurities.

Bi_2Te_3 has been found as one of the 3D TIs in the previous experimental work. The surface state of both the pure Bi_2Te_3 and the Sn-doped Bi_2Te_3 was confirmed by angle-resolved photoemission spectroscopy (ARPES) and magnetotransport measurements [4], [17]. Moreover, the AHE of Cr- and Mndoped Bi_2Te_3 was reported in [7], [11], and [14]. However, the application and the properties of Mn-doped Bi_2Te_3 as HE sensors are not well studied. In this paper, we fabricate the HE sensors based on Mn-doped Bi_2Te_3 TI thin films. Both HE and AHE sensors are systematically studied by varying the Mn concentration. The influence of the Mn concentration on sensitivity of $Mn_xBi_{2-x}Te_3$ HE sensors will be discussed.

II. Experiment

A. Thin film deposition

$Mn_xBi_{2-x}Te_3$ thin films with Mn concentration in the range from 0 to 0.25 were grown by Perkin–Elmer 430 molecular beam epitaxy system on mica substrates. When x > 0.25, the Mn-doping tends to breakdown the epitaxial growth. The mica substrate was cleaved freshly before the depositions. Source materials (Mn, Bi, and Te) with high purity were loaded in Knudsen effusion cells. The base pressure during growth was kept as ~8 × 10−9 torr. The quality of the thin films during growth was monitored by reflection high-energy electron diffraction (RHEED). The thin films with the thickness of 15 nm were grown. To reduce Te vacancies, the temperature of Bi and Te source materials was adjusted to obtain a Te-rich environment. The doping concentration of Mn in Bi2Te3 thin films was controlled by adjusting its cell temperature.

Corresponding author: Z. Zhang (e-mail: zhenzisu@iastate.edu).

B. Hall effect sensor fabrication and characterization

The HE sensors were fabricated with two major steps. First, the as-grown thin films were fabricated into 1 mm-wide Hall bar geometry [Fig. 2(d)] by the reactive-ion etching method. Ar was used as etching gas. During the etching process, the flow rate of Ar was kept as 20 sccm; and the power was kept as 100 W. Second, the HE sensors were fabricated by attaching Au wire to the contact pad to form the ohmic contact. The composition analysis of sensors was carried out at the FEI Quanta FE-EDX. The Mn concentrations were confirmed and the three different Mn-doping levels in MnxBi2−xTe3 were selected as x = 0.01, 0.08, and 0.23. The crystal structure of sensors was studied by X-ray spectrometer [Siemens D500 X-ray diffraction (XRD) system]. The topography of sensors was characterized using atomic force microscopy (AFM) in a tapping mode. The magnetotransport properties of sensors were characterized in quantum design physical properties measurement system. The measuring geometry is shown in Fig. 2(d). The Hall resistance under low magnetic field (from −0.2 to 0.2 T) normal to the surface of thin-film sensors was tested. The applied ac current was kept as 0.05 mA with frequency as 19 Hz.

III. Results and Discussion

A. Crystal structure of $Mn_xBi_{2-x}Te_3$ Hall effect sensors

Fig. 1 shows the XRD profiles of $Mn_xBi_{2-x}Te_3$ HE sensors. Two sets of diffraction peaks are observed. One set of these diffraction peaks can be indexed as the {001} family plane of mica substrate, while (0015), (0018), and (0021) diffraction peaks are obtained from $Mn_xBi_{2-x}Te_3$ thin films with the rhombohedral structure. The visibility of diffraction peaks from the mica substrate in all samples is due to the low thickness of thin films (∼15 nm) in comparison with the penetration depth of X-rays. This diffraction pattern indicates that the mica substrate is cleaved along its ab plane, while $Mn_xBi_{2-x}Te_3$ thin film is preferentially deposited along its c-axis. Moreover, except {001} family peaks, no extra peaks from MnxBi2−xTe3 thin films are observed in three doping levels, indicating that thin films being utilized to fabricate sensors are grown epitaxially and highly orientated.

The c-axis lattice constant of $Mn_xBi_{2-x}Te_3$ thin films with x = 0.01, calculated from the (0018) diffraction peak in Fig. 1(a), is 30.54 Å. Comparing with undoped Bi_2Te_3 (c = 28.84 Å) [9], the c lattice constant of the Mn-doped thin films increases. Moreover, with Mn concentration increasing to x = 0.23, the c lattice constant of $Mn_xBi_{2-x}Te_3$ increases to 30.61 Å. Since the ionic radius of Mn is smaller than Bi, the changes in lattice constant with doping Mn shows that Mn not only substitutes into the Bi site but is also trapped in the van der Waals gap between the quintuple layers [15]. In Fig. 1(c), the (0021) diffraction peak of $Mn_xBi_{2-x}Te_3$ with x = 0.23 becomes slightly broad compared with the less doped samples. This may also result from the lattice distortions induced by Mn atoms.

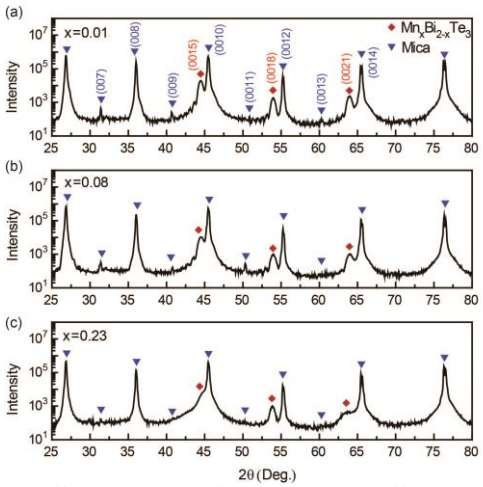

Fig. 1. X-ray diffraction patterns of $Mn_xBi_{2-x}Te_3$ Hall effect sensor fabricated on mica substrate with (a) x = 0.01, (b) x = 0.08, and (c) x = 0.23, where diffraction peaks from mica substrate and $Mn_xBi_{2-x}Te_3$ thin film are indexed in blue and red, respectively.

B. Surface morphology of $Mn_xBi_{2-x}Te_3$ Hall effect sensors

Fig. 2 shows the AFM images of $Mn_xBi_{2-x}Te_3$ thin- film HE sensors with x = 0.01, 0.08, and 0.23. With the low Mn concentration x = 0.01 [Fig. 2(a)], the sample shows the terrace structure with the terrace width range from 200 to 500 nm. Moreover, the height of each terrace is ∼1 nm, which is the same as the thickness of one QL of $Mn_xBi_{2-x}Te_3$. These large surface terraces, therefore, indicate a layer-by-layer growth mechanism of the Mn-doped Bi_2Te_3 on the mica substrate.

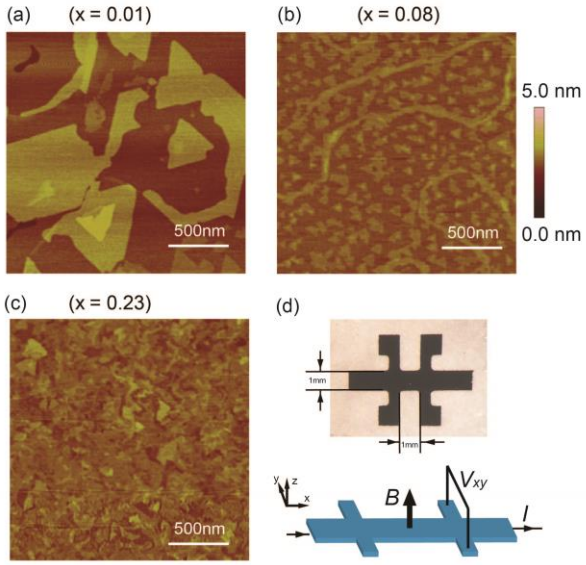

Fig. 2. (a), (b), and (c) Surface morphology of $Mn_xBi_{2-x}Te_3$ thin films with x= 0.01, x=0.08, and x=0.23, respectively, (d) Hall effect sensor fabricated with $Mn_xBi_{2-x}Te_3$ thin films, and geometry of Hall effect measurement.

With increasing Mn concentration to x = 0.08 and 0.23 [Fig. 2(b) and (c)], terrace structure still exists. Moreover, streak lines were observed for all the samples in the in situ RHEED patterns. It is indicated that the thin films with high Mn concentration retain epitaxy. Fig. 2(a)–(c) further shows that with increasing Mn concentration, the width of surface

terraces decreases. The reducing of surface terrace and slightly roughening of the sensor surface may result from the chemical disorder due to competition of Mn and Bi atoms at Bi site as well as the lattice distortions due to Mn atoms trapped in QL gaps. The root mean square (rms) surface roughness of sensors shows low values for all samples. The highest rms roughness of sensors is 0.2 nm when x = 0.23, which is much smaller than the previous report of Cr-doped Bi2Te3 [7]. The low roughness and high quality of $Mn_xBi_{2-x}Te_3$ thin films consolidate the following results of the electric transport properties of sensors.

C. Electric transport properties of $Mn_xBi_{2-x}Te_3$ Hall effect sensors

The transport responses of $Mn_xBi_{2-x}Ti_3$ HE sensors with x = 0.01, 0.08, and 0.23 are shown in Fig. 3. Hall resistance for all the three sensors shows the tendency of decrease with increasing magnetic field. The negative slope of the Hall resistance indicates the Mn-doped Bi2Te3 sensors remain n-type. The carrier density of sensors at 30 K is calculated using n = (|RH |e) −1 , where RH is the Hall coefficient and e is the electron charge. The calculated carrier density decreases from 9.5 × 1019 to 7.5 × 1019 cm−3 at 30 K as Mn concentration increases from x = 0.01 to 0.23, reflecting the downward motion of Fermi level (E_F). The relative large carrier density of sensors compared with ideal TIs indicates that the sensors are heavily donor-doped. As a result, E_F is far above the surface Dirac point. Such a band structure is consistent with other TIs, such as $Sb_xBi_{2-x}Te_3$ [16]. The carrier mobility of $Mn_xBi_{2-x}Ti_3$ sensor was calculated using $\mu = {}^{\sigma_{xx}}/_{ne}$, where σ_{xx} is the longitudinal conductivity. The mobility value calculated at 30 K varies with the changing Mn concentration. At low doping level (x = 0.01), the carrier mobility is 473.5 cm2/Vs. The carrier mobility decreases to 72.4 cm2/Vs in highly doped sensors with x = 0.23. The lower carrier mobility in $Mn_xBi_{2-x}Te_3$ sensors than the reported value in pure Bi_2Te_3 (5800 cm2/Vs) [17] indicates that the incorporation of Mn destroys the massless surface state of topological insulators. We will show in the following that AHE is also induced in heavily doped $Mn_xBi_{2-x}Te_3$.

At low doping level with x = 0.01 [Fig. 3(a)], the sensor shows ordinary HE. The overlap of straight lines of the Hall resistance at different temperatures indicates the temperature independence of HE for this composition. For the sensor with Mn concentration x = 0.23 [Fig. 3(c)], the temperature dependence of the Hall resistance becomes more obvious than others, and the AHE occurs during cooling. At high temperature, Hall resistance shows linear dependence on magnetic field. However, the Hall resistance exhibits hysteresis when the temperature is lower than 12.5 K, indicating the occurrence of a ferromagnetic phase transition [14]. Simultaneously, the Hall resistance of sensors under a magnetic field of −0.2 T increases. Moreover, the hysteresis in Hall resistance increases with further cooling, being similar to the temperature dependence of ferromagnetic materials [18]. The corresponding coercive field H_c as a function of temperature is shown in Fig. 3(d). H_c abruptly increases around 12.5 K indicating that the ferromagnetic transition temperature Tc of sensors is near 12.5 K, which is in the same temperature range as in [11] and [12]. The temperature dependence of longitudinal resistance ($R/R_{30\ K}$) of sensors at various Mn concentrations is further depicted in Fig. 3(d) (inset). The typical metallic behavior can be observed for x = 0.01. However, the resistance curve of sensor with x = 0.23 shows a dip around 15 K, similar to its Curie temperature T_c. With the temperature lower than 15 K, the sensor shows the similar resistance behavior as semiconductors.

For x = 0.08, a broad dip is observed in $R/R_{30\ K}$ [Fig. 3(d) (inset)] at ∼10 K. Below 10 K, the Hall resistance [Fig. 3(b)] starts to show a nonlinear behavior. However, there is no ferromagnetic transition, since no hysteresis is observed. This indicates that Mn concentration is not sufficient to induce the long-range-ordered ferromagnetic transition.

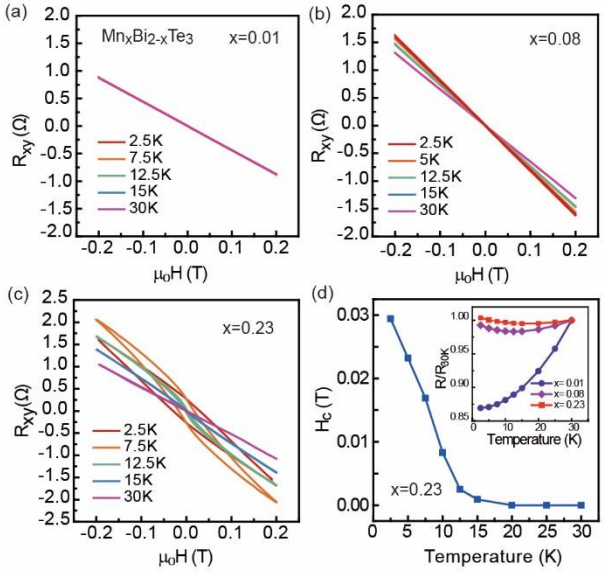

Fig. 3. Temperature dependence of Hall resistance curves under low magnetic field for $Mn_xBi_{2-x}Te_3$ Hall effect sensor with (a) x=0.01, (b) x = 0.08, and (c) x=0.23. (d) Temperature dependence of coercive field for $Mn_xBi_{2-x}Te_3$ Hall effect sensor with x=0.23. Inset shows the temperature dependent of longitudinal resistance (R/R_{30K}) of sensors at various Mn concentration.

D. The effect of temperature and Mn concentration on sensitivity of $Mn_xBi_{2-x}Te_3$ Hall effect sensors

Sensitivity is the most important figure of merit for Hall sensor. For the linear behavior of ordinary Hall effect, Hall resistivity of sensors can be expressed as However, for AHE since the hysteresis is superimposed on the linear Hall effect behavior, Hall resistance is described by, which is composed of both ordinary Hall resistivity and anomalous Hall resistivity. The sensitivity of Hall effect sensors can be defined as. Based on the electric transport properties shown in Fig. 2, sensitivity of sensors close to 0 T is calculated using the above equation for $Mn_xBi_{2-x}Te_3$ sensors (x = 0.01, 0.08, 0.23).

Sensitivity is the most important figure of merit for the Hall sensor. For the linear behavior of ordinary HE, Hall resistivity of sensors is expressed as $\rho_{xy} = R_H H$. For AHE, Hall resistance is described as $\rho_{xy} = R_H H + R_{\mathrm{AH}}(M)$, which is

composed of both ordinary Hall resistivity $R_H H$ and anomalous Hall resistivity $R_{\mathrm{AH}} M$. The sensitivity of HE sensors can be defined as $S = d\rho_{xy}/dH_{\perp}$. Based on the magnetotransport properties shown in Fig. 3, the sensitivity of sensors close to 0 T is calculated using the above equation.

Figure 4 shows the dependence of sensitivity of sensor on temperature and Mn concentration. Sensitivity of sensors with Mn concentration x = 0.01 and 0.08 is about 5 Ω/T, being a nearly flat line at various temperatures. For sensors with Mn concentration x = 0.23, sensitivity increases to 45 Ω/T when the temperature is lower than T_c. This sensitivity is higher than most ultrathin metals such as Ni and Co [19]. Moreover, Figs. 3 and 4 shows that the increase in sensitivity of sensors is due to AHE caused by the occurrence of ferromagnetic phase transition in strongly Mn doped sensors. Fig. 4 further shows that highest sensitivity can be obtained around ferromagnetic temperature T_c. The relative low sensitivity together with high carrier density in these sensors implies the bulk carriers in TI significantly contribute to Hall resistance [16]. It is promising to further increase the sensitivity by decreasing the carrier density with band structure engineering and gate control method.

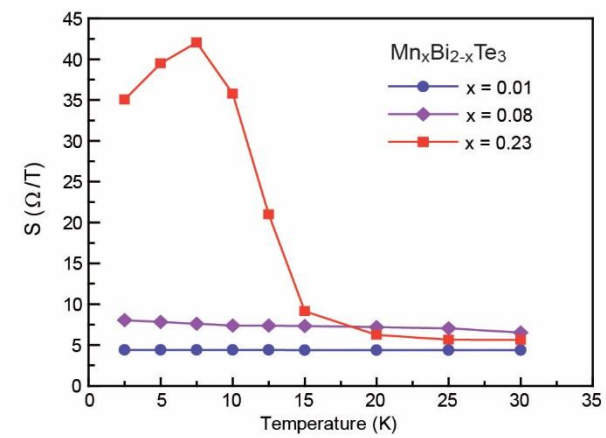

Fig. 4. The effect of temperature and Mn concentration on Hall sensitivity of $Mn_xBi_{2-x}Te_3$ Hall effect sensor with x = 0.01, 0.08, and 0.23.

IV. Conclusion

In summary, a detailed study on the influence of Mn concentration on transport response and sensitivity of $Mn_xBi_{2-x}Te_3$ Hall effect sensors are presented. Surface and crystal characterization shows that the sensors are fabricated with high quality $Mn_xBi_{2-x}Te_3$ thin films. For heavily Mn doped sensors with x = 0.23, anomalous Hall effect is observed when cooling the temperature to 12.5 K. As a result, an improvement on Hall sensitivity is found. The Hall sensitivity of sensors with $Mn_xBi_{2-x}Te_3$ x = 0.23 is 45 Ω/T, being 8 times higher than that of sensors with x = 0.08 and 0.01. Our work will be helpful to design TIs based Hall effect sensors.

Acknowledgment

This work was supported by the U.S. National Science Foundation Division of Electrical, Computer and Communications Systems (ECCS) under Award 1201883. The work at Ames Laboratory was supported by the U.S. Department of Energy (DOE), Office of Science, Basic Energy Sciences, Materials Science and Engineering Division. The research was performed at the Ames Laboratory, which is operated for the U.S. DOE by Iowa State University under Contract DE-AC02-07CH11358.

References

[1] E. Ramsden, *Hall-effect sensors: theory and application*, Newnes: Burlington, 2006.

[2] R. S. Popovic, *Hall effect devices*, CRC Press, 2003.

[3] J. E. Moore, "The birth of topological insulators," *Nature*, vol. 464, pp. 194-198, 2010.

[4] Y. Chen, J. Analytis, J.-H. Chu, Z. Liu, S.-K. Mo, X.-L. Qi, H. Zhang, D. Lu, X. Dai, and Z. Fang, "Experimental realization of a three-dimensional topological insulator Bi_2Te_3," *Science*, vol. 325, pp. 178-181, 2009.

[5] V. Kulbachinskii, A. Y. Kaminskii, K. Kindo, Y. Narumi, K. Suga, P. Lostak, and P. Svanda, "Ferromagnetism in new diluted magnetic semiconductor $Bi_{2-x}Fe_xTe_3$," *Physica B: Condens. Matter*, vol. 311, pp. 292-297, 2002.

[6] M. Z. Hasan and C. L. Kane, "Colloquium: topological insulators," *Rev. Mod. Phys.*, vol. 82, p. 3045, 2010.

[7] L. Bao, W. Wang, N. Meyer, Y. Liu, C. Zhang, K. Wang, P. Ai, and F. Xiu, "Quantum Corrections Crossover and Ferromagnetism in Magnetic Topological Insulators," *Sci. Rep.*, vol. 3, 2013.

[8] Y, Ni, Z. Zhang, C. I. Nlebedim, R. L. Hadimani, G. Tuttle, D. C. Jiles, "Ferromagnetism of Magnetically Doped Topological Insulators in $Cr_xBi_{2-x}Te_3$ Thin Films," *J. Appl. Phys.*, In press, 2015.

[9] X. Chen, H. Zhou, A. Kiswandhi, I. Miotkowski, Y. Chen, P. Sharma, A. L. Sharma, M. Hekmaty, D. Smirnov, and Z. Jiang, "Thermal expansion coefficients of Bi_2Se_3 and Sb_2Te_3 crystals from 10 K to 270 K," *Appl. Phys. Lett.*, vol. 99, p. 261912, 2011.

[10] J. Choi, S. Choi, J. Choi, Y. Park, H. M. Park, H. W. Lee, B. C. Woo, and S. Cho, "Magnetic properties of Mn-doped Bi_2Te_3 and Sb_2Te_3," *Phys. Status Solidi (b)*, vol. 241, pp. 1541-1544, 2004.

[11] J. Bos, M. Lee, E. Morosan, H. Zandbergen, W. Lee, N. Ong, and R. Cava, "Ferromagnetism below 10 K in Mn-doped BiTe," *Phys. Rev. B*, vol. 74, p. 184429, 2006.

[12] C. -Z. Chang *et al.*, "Study of the structural, electric and magnetic properties of Mn-doped Bi_2Te_3 single crystals," *New J. Phys.*, vol. 15, p. 103016, 2013.

[13] C.-Z. Chang, J. Zhang, X. Feng, J. Shen, Z. Zhang, M. Guo, K. Li, Y. Ou, P. Wei, and L.-L. Wang, "Experimental observation of the quantum anomalous Hall effect in a magnetic topological insulator," *Science*, vol. 340, pp. 167-170, 2013.

[14] D.-X. Qu, Y. Hor, J. Xiong, R. Cava, and N. Ong, "Quantum oscillations and Hall anomaly of surface states in the topological insulator Bi_2Te_3," *Science*, vol. 329, pp. 821-824, 2010.

[15] J. Růžička, O. Caha, V. Holý, H. Steiner, V. Volobuiev, A. Ney, G. Bauer, T. Duchoň, K. Veltruská, and I. Khalakhan, "Structural and electronic properties of manganese-doped Bi_2Te_3 epitaxial layers," *New J. Phys.*, vol. 17, p. 013028, 2015.

[16] J. Zhang, C.-Z. Chang, Z. Zhang, J. Wen, X. Feng, K. Li, M. Liu, K. He, L. Wang, and X. Chen, "Band structure engineering in $(Bi_{1-x}Sb_x)_2Te_3$ ternary topological insulators," *Nat. Commun.*, vol. 2, p. 574, 2011.

[17] K. Wang, Y. Liu, W. Wang, N. Meyer, L. Bao, L. He, M. Lang, Z. Chen, X. Che, and K. Post, "High-quality Bi_2Te_3 thin films grown on mica substrates for potential optoelectronic applications," *Appl. Phys. Lett.*, vol. 103, p. 031605, 2013.

[18] Y. Ni, Z. Zhang, C. I. Nlebedim, and D. C. Jiles, "Influence of Ga-concentration on the electrical and magnetic properties of magnetoelectric $CoGa_xFe_{2-x}O_4/BaTiO_3$ composite," *J. Appl. Phys.*, vol. 117, p. 17B906, 2015.

[19] A. Gerber and O. Riss, "Perspective of spintronics applications based on the extraordinary hall effect," *J.Nanoelectron. Optoe.*, vol. 3, pp. 35-43, 2008.

[20] F. Xiu et al., "Quantum capacitance in topological insulators," Sci. Rep., vol. 2, Sep. 2012, Art. ID 669.